Molecular Cancer Therapeutics

In Vitro and *In Vivo* Efficacy of a Novel CD33-Targeted Thorium-227 Conjugate for the Treatment of Acute Myeloid Leukemia

Urs B. Hagemann, Katrine Wickstroem, Ellen Wang, Adam O. Shea, Kristine Sponheim, Jenny Karlsson, Roger M. Bjerke, Olav B. Ryan, and Alan S. Cuthbertson

Abstract

The clinical efficacy of the first approved alpha pharmaceutical, Xofigo (radium-223 dichloride, $^{223}RaCl_2$), has stimulated significant interest in the development of new alpha-particle emitting drugs in oncology. Unlike radium-223 (^{223}Ra), the parent radionuclide thorium-227 (^{227}Th) is able to form highly stable chelator complexes and is therefore amenable to targeted radioimmunotherapy. We describe the preparation and use of a CD33-targeted thorium-227 conjugate (CD33-TTC), which binds to the sialic acid receptor CD33 for the treatment of acute myeloid leukemia (AML). A chelator was conjugated to the CD33-targeting antibody lintuzumab via amide bonds, enabling radiolabeling with the alpha-emitter ^{227}Th. The CD33-TTC induced *in vitro* cytotoxicity on CD33-positive cells, independent of multiple drug resistance (MDR) phenotype. After exposure to CD33-TTC, cells accumulated DNA double-strand breaks and were arrested in the G_2 phase of the cell cycle. *In vivo*, the CD33-TTC demonstrated antitumor activity in a subcutaneous xenograft mouse model using HL-60 cells at a single dose regimen. Dose-dependent significant survival benefit was further demonstrated in a disseminated mouse tumor model after single dose injection or administered as a fractionated dose. The data presented support the further development of the CD33-TTC as a novel alpha pharmaceutical for the treatment of AML. *Mol Cancer Ther; 15(10); 2422–31.* ©*2016 AACR.*

Introduction

Xofigo (radium-223 dichloride, $^{223}RaCl_2$) is the first in-class alpha pharmaceutical approved for the treatment of metastatic castration-resistant prostate cancer (1). The inherent bone-seeking properties of radium-223 (^{223}Ra; see ref. 2) allows for the effective delivery to bone metastases. The lack of suitable complexing agents for ^{223}Ra limits its use for tumor-targeting moieties, such as antibodies, and hence broader utility in oncology (3). In contrast, thorium-227 (^{227}Th), the parent radionuclide of ^{223}Ra, can be readily complexed by octadentate chelates of the 3,2 hydroxypyridinone (3,2-HOPO) class. These 3,2-HOPO chelates, complexed with ^{227}Th, can further be attached to tumor-targeting antibodies, referred herein as targeted thorium-227 conjugates (TTC). TTCs have the potential to deliver the high potency of the alpha-particle to a multitude of different cancer types, including those of the lympho-hematopoietic system.

Acute myeloid leukemia (AML) is a rare, highly malignant neoplasm with a poor survival prognosis and results in a high number of cancer-related deaths. The age-adjusted incidence rate of AML in the United States in the years 1975 to 2003 was 3.4 per 100,000 persons and the disease accounted for about 25% of all leukemia in the Western world (4). Despite the high unmet medical need, the pace of new drug approvals for AML in recent years has remained almost at a standstill. The antibody–drug conjugate (ADC) gemtuzumab ozogamicin (GO; Mylotarg) targeting the CD33-positive leukemic blasts, initially approved by the FDA in 2001 was later withdrawn from the market in 2009 due to lack of prespecified overall improvement in outcome, along with drug-related toxicities (5, 6). Although many strategies are currently being assessed which attempt to target the genetic heterogeneity of AML, including hypomethylating agents, fms-related kinase inhibitors, and many combination therapies, there is still need for new effective drugs for the treatment of AML (7).

Recently, preclinical and clinical development has focused on two new antibody drug conjugates (ADC), SGNCD33A (8) and IMGN779 (9), both currently being tested in clinic trials. Furthermore, AMG330, a CD33/CD3-directed bispecific T-cell engager antibody (BiTE; refs. 10–13), has entered clinical testing and chimeric antigen receptors T-cell approaches (CAR-T) are additionally feeding the pipeline for the treatment of AML (14, 15). All of these immunotherapeutic agents are targeting the sialoadhesin receptor CD33 (Siglec-3), a 67-kDa protein, expressed on leukemic blasts of AML patients (16). Lintuzumab, a humanized anti-CD33 IgG1 antibody (17, 18), although well-tolerated in AML patients, showed only modest activity even at doses capable of completely saturating CD33-binding sites (19). Furthermore, AVE9633, an anti-CD33 antibody coupled to a maytansinoid derivative, and an immunotoxin conjugate, that is, HuM-195/rGel, lintuzumab linked to gelonin, were evaluated in clinical phase I trials and showed only modest activity (20, 21).

Thorium Conjugate Research, Bayer AS, Oslo, Norway.

Note: Supplementary data for this article are available at Molecular Cancer Therapeutics Online (http://mct.aacrjournals.org/).

Corresponding Author: Urs B. Hagemann, Thorium Conjugate Research, Bayer AS, Drammensveien 288, Oslo 0283, Norway. Phone: 472-313-0584; Fax: 472-313-0583; E-mail: urs.hagemann@bayer.com

doi: 10.1158/1535-7163.MCT-16-0251

An alternative to antibody–drug conjugates or immunotoxins is radioimmunotherapy which capitalizes on the radiosensitivity of AML (22, 23). Radioimmunotherapy has the potential added benefit of overcoming chemoresistance induced by multi-drug resistance pumps (24, 25). As such, lintuzumab has been evaluated as radioimmunoconjugate with the beta-emitter iodine-131 (^{131}I) and with the alpha-emitters bismuth-213 (^{213}Bi) and actinium-225 (^{225}Ac) (26). Early clinical studies using ^{131}I-lintuzumab demonstrated the clinical potential of radioimmunotherapy in AML (27), but also highlighted limitations of this approach due to radiolysis of the drug product and off-target toxicity caused by the long range of γ-radiation. Off-target toxicity can potentially be reduced by using high-energy, short-range alpha-emitters (range in tissue of approximate 50–80 μm) which are characterized by their high linear energy transfer (LET; ref. 28). Even though ^{213}Bi-lintuzumab, when used as single agent or in combination with conventional chemotherapy, demonstrated acceptable safety and antileukemic activity (29, 30), its use in clinic is challenging due to the short half-life of ^{213}Bi (46 minutes). In contrast, ^{225}Ac has a half-life of 10 days and ^{225}Ac-lintuzumab (Actimab A) and demonstrated antileukemic activity as a single agent or in combination with conventional chemotherapy in clinical trials at doses of $\leq$111 kBq/kg (31, 32).

We present the development of a CD33-targeted thorium-227 conjugate (CD33-TTC), comprising the CD33 monoclonal antibody lintuzumab, an octadentate 3,2-HOPO chelate (33), conjugated to the antibody allowing radiolabeling with the alpha-emitter thorium-227. Thorium-227 has a half-life of 18.7 days and is purified from an actinium-227 generator. In the decay chain of thorium-227, a total of five high-energy daughter alpha-particles (^{223}Ra, ^{219}Rn, ^{215}Po, ^{211}Bi, and ^{211}Po) and two beta decays (^{211}Pb and ^{207}Tl) are generated, with ^{211}Pb as the final stable end product (ref. 34; Supplementary Fig. S1). The presented preclinical data support the further development of this new class of targeted alpha pharmaceutical for the treatment of AML.

Materials and Methods

Cells

HL-60, KG-1, and Ramos cells were obtained from ATCC. All cell lines were authenticated using by the manufacturer. The cell lines were purchased within the period of 2008–2015, characterized by the vendor (PCR fingerprinting), and no further cell line authentication was conducted by the authors. Cells were maintained in an incubator of 5% CO_2 at 37°C. HL-60 and KG-1 cells were cultured in IMDM with 20 % FCS and 1% penicillin and 1% streptomycin. Ramos cells were cultured in RPMI1640 with 10% FCS and 1% penicillin and 1% streptomycin.

Expression, purification, and conjugation of the CD33 antibody–chelator conjugate

The gene encoding the CD33 antibody lintuzumab was synthesized (GeneArt/Life Technologies) and cloned into a plasmid enabling expression in CHO-K1 cells. The CD33 antibody was harvested from the cell culture and purified via an affinity MAbSelectSure column (GE Healthcare) followed an anion exchange chromatography column (QFF Sepharose; GE Healthcare) and a cation exchange chromatography column (Poros XS; Life Technologies) to remove high-molecular weight fractions and in-process impurities. The antibody was filtered through a 0.22-μm filter (Millipore), formulated in PBS, pH 7.2 and stored at −64°C. All work was conducted by Cobra Biologics (Sweden).

The synthesis of the 3,2-HOPO chelator is described elsewhere (33) and was conducted by Synthetica (Norway).

Conjugation of the 3,2-HOPO chelator to lysine residues within the CD33 antibody and an isotype control was achieved through *in situ* activation of the chelator using EDC/NHS chemistry and subsequent incubation with the antibody in PBS, pH 7.0, for 60 minutes at room temperature. The resulting antibody–chelator conjugates were purified by size-exclusion chromatography (SEC; HiLoad 16/600 Superdex 200; GE Healthcare) and stored at −20°C.

The chelator to antibody ratio (CAR) was determined by SEC (TSKgel SUPER SW 3000 column; Tosoh) by monitoring the absorbance of the CD33 antibody–chelator conjugate at 280 and 335 nm. The CAR value was calculated using the following formula: CAR = extinction coefficient of mAb (335 nm) − ratio × extinction coefficient of mAb (280 nm)/ratio × extinction coefficient of chelator (280 nm) − extinction coefficient of chelator (335 nm).

Radiolabeling and characterization of the CD33-TTC

Thorium-227 was purified from an actinium-227 generator as described previously (35). Two hundred and fifty micrograms of CD33 antibody–chelator conjugate were mixed with ^{227}Th-activities, ranging from 0.2 to 2.5 Mbq and incubated at room temperature for 60 minutes. Radiochemical purity (RCP) was determined by instant thin-layer chromatography (iTLC). For radiostability testing, the CD33-TTC was analyzed over the course of 48 hours by iTLC and SEC.

The immunoreactive fraction (IRF) was determined after Lindmo (36). Recombinant human CD33 (Novus Biologicals) or BSA (Sigma) was coated to tosyl-activated magnetic beads (Dynabeads M-280; Life-Technologies). Fifty becquerel of CD33-TTC/sample [measured on an HPGe counter (GEM; Perkin Elmer)] were incubated for 1.5 hours at 37°C on a titration of 1.5 to 25 million beads of either CD33- or BSA-coated beads. Beads were sorted on a magnetic rack and the radioactivity in the supernatant and on the bead pellets was determined. The IRF was calculated as the fraction of activity bound to CD33-coated beads subtracting the unspecific activity measured on BSA-coated beads.

Internalization of the CD33-TTC was compared with an isotype control-TTC as described previously (37). HL-60 cells (400,000/mL) were incubated in presence of 1 μg of CD33-TTC or isotype control-TTC (radiolabeled at a specific activity of 20 kBq/μg) at 37°C with 5% CO_2. Cells were pelleted by centrifugation at different timepoints (30, 60, 120, and 240 minutes, and 6 and 24 hours). The radioactivity in the cell pellets was recorded using a gamma counter (Wizard/Perkin Elmer) and counts per minute were plotted against time to monitor internalization.

Binding potency to CD33 by ELISA and FACS analysis

Recombinant human CD33 (Novus Biologicals) was coated to ELISA plates (1 μg/mL; NUNC/Maxisorp). Wells were blocked with skim milk [4 % (w/v)]. CD33 antibody, CD33 antibody–chelator conjugate, an isotype antibody–chelator conjugate, and CD33-TTC (radiolabeled at a specific activity of 50 kBq/μg) were titrated (1:3; 100 μg/mL) on the CD33-coated ELISA plate. Unbound samples were washed off and bound samples were visualized using horseradish peroxidase–labeled anti-human kappa-HRP antibody (Southern Biotech), followed by incubation

with 1-step TMB blotting solution (Thermo Scientific Pierce). The reaction was stopped by addition of 1 mol/L HCl. The absorbance was measured at 450 nm in a plate reader (Perkin Elmer). EC_{50} values were calculated using GraphPad Software.

CD33-expresisng HL-60 cells (200,000 cells/well) were incubated in presence of serial dilutions (1:3; 100 μg/mL) of CD33 antibody, CD33 antibody–chelator conjugate or an isotype antibody-chelator conjugate. Unbound samples were washed off and bound samples were detected using PE-labeled anti-human IgG (Biolegend). Mean fluorescence intensities (MFI) were recorded using a Quanta SC MPL machine (Beckman Coulter). EC_{50} values were calculated using GraphPad software.

Measurement of cell viability and cell-cycle arrest

CD33 receptor densities on HL-60, KG-1, and Ramos cells were determined using QiFiKit (Dako). Cells were seeded into 24-well culture plates (200,000 cells/mL). CD33-TTC, an isotype control-TTC (both radiolabeled at a specific activity of 50 kBq/μg) and CD33 antibody–chelator conjugate were incubated on the cells for 4 hours at 37°C at activities ranging from 0 to 20 kBq/mL. Cells were washed and reseeded into a new 24-well culture plate. At different timepoints, cells were harvested and the viability was measured using CellTiterGlo kit (Promega). The cell viability was expressed in percent by normalization to cells grown in medium only. DNA double-strand breaks were determined using AlexaFluor 647–labeled anti-phospho-Histone H2A.X antibody (Cell Signaling Technology). Cells were costained with an AlexaFluor 488–labeled anti-cleaved caspase-3 antibody (Cell Signaling Technology) to detect no-apoptotic cells. Cell-cycle analysis was analyzed using the apoptosis, DNA damage, and cell proliferation kit (ADDCP; BD Biosciences). FACS analysis was performed using a Quanta SC MPL instrument (Beckman Coulter).

Animal models

All animal models were conducted at Pipeline Biotech and were in accordance with the Danish animal welfare law, approved by local authorities. In all studies, animals received an intraperitoneal (i.p.) injection of an unrelated murine IgG2a antibody (200 μg/animal; UPC10; Sigma) 24 hours prior treatment to block unspecific spleen uptake (38).

In vivo biodistribution

Five million HL-60 cells, suspended in 0.1 mL 50% Matrigel (BD Biosciences), were inoculated subcutaneously into 6 mice per group (female/NMRI nu/nu mice/Taconic, Europe). At an average tumor volume of 200–300 mm^3, animals were administered with a single intravenous injection of CD33-TTC (500 kBq/kg; protein dose of 0.36 mg/kg). Tumors and organs were harvested at $t = 24$ hours, $t = 4$ days, and $t = 7$ days. Radioactivities were counted using an HPGe detector linked to an autosampler (Gamma Data) at Bayer AS. Thorium-227 and ^{223}Ra activities were decay corrected to the timepoint of injection and plotted in Bq/g.

In vivo efficacy models

Five million HL-60 cells, suspended in 0.1 mL 50% Matrigel (BD Biosciences), were inoculated subcutaneously into 10 mice per group (female/NMRI nu/nu mice/Taconic). At an average tumor volume of 70–100 mm^3, animals received either a single intravenous injection of CD33-TTC or isotype control-TTC (radioactive dose of 700 kBq/kg; protein dose of 0.36 mg/kg), CD33 antibody–chelator conjugate (0.36 mg/kg) or vehicle. Body weights were measured biweekly. Tumor growth was calculated using the formula: $V = 0.5 \times (\text{length} + \text{width})^2$. Animals were sacrificed by cervical dislocation upon reaching the humane endpoint (tumor volume $\geq$ 1,500 mm^3; body weight loss $\geq$ 20%).

In the disseminated tumor model, female C.B-17 SCID mice (Taconic) were injected intravenously with 5,000,000 HL-60 cells. At study day 5, animals received a single intravenous injection of CD33-TTC at radioactivity doses of 50, 150, or 300 kBq/kg (protein dose of 0.04 mg/kg). An additional treatment group received a second intravenous injection of CD33-TTC at a dose of 150 kBq/kg (day 19). Control groups received a single intravenous injection of an isotype control-TTC (radioactivity dose of 300 kBq/kg; 0.04 mg/kg), CD33 antibody–chelator conjugate (0.04 mg/kg), or vehicle. White and red blood cell counts were determined (Vet ABC analyzer) at study day -1 (vehicle), day 67, and at day 123 (end of study). Animals were sacrificed by cervical dislocation upon reaching humane endpoints defined by clinical signs of disease including palpable tumors, scruffy fur, weight loss, and hind leg paralysis. Diseased organ samples were isolated and analyzed for CD33 (Novacastra) and CD45 (Dako) expression by IHC on paraffin-embedded tissue sections (TISSUE-TEK/ Miles Scientific) at Micromorph (Sweden). Survival plots were generated using GraphPad software. Statistical analysis was performed using a log-rank (Mantel–Cox) test and was considered to be significant at $P < 0.05$.

Results

Preparation and characterization of the CD33-TTC

The cDNA sequence of the CD33 antibody lintuzumab was derived from the literature (18). Standard molecular biology techniques were used, enabling recombinant expression in CHO-K1 cells and subsequent purification as described previously. In parallel, the 3,2-HOPO chelator was synthesized (33), capable of binding the radionuclide ^{227}Th at one end, and carrying a reactive NHS-group at the other end to enable conjugation of the chelator to free lysine residues in the CD33 antibody, thereby forming stable amide bonds. A schematic presentation of the resulting CD33-TTC is presented in Fig. 1A. A chelator to antibody ratio (CAR) of 0.8 chelator molecules per antibody was determined by size-exclusion chromatography by monitoring the UV signal at 280 nm for protein absorbance and at 335 nm for chelator absorbance in parallel.

The radiolabeling properties of the CD33 antibody–chelator conjugate were studied in more detail. The CD33 antibody–chelator conjugate was incubated with ^{227}Th at room temperature for $\geq$60 minutes. The radiochemical purity (RCP), defined as the amount of bound ^{227}Th in the final CD33-TTC product, was determined by iTLC to be consistently $\geq$95%. Furthermore, the CD33-TTC demonstrated high RCP and only slight increase in high-molecular weight fractions when stored for 48 hours at room temperature (Fig. 1B), enabling *in vivo* applications.

The binding properties of the CD33 antibody, the CD33 antibody–chelator conjugate, and the CD33-TTC were subsequently tested. No significant loss in binding affinity to recombinant human CD33 due to conjugation or radiolabeling was observed by ELISA analysis (Fig. 2A). Similarly, no loss in binding affinity to CD33 expressed on HL-60 cells was observed by FACS analysis (Supplementary Fig. S2). Determination of the immunoreactive fraction (IRF) for CD33-TTC demonstrated that $\geq$95% of the

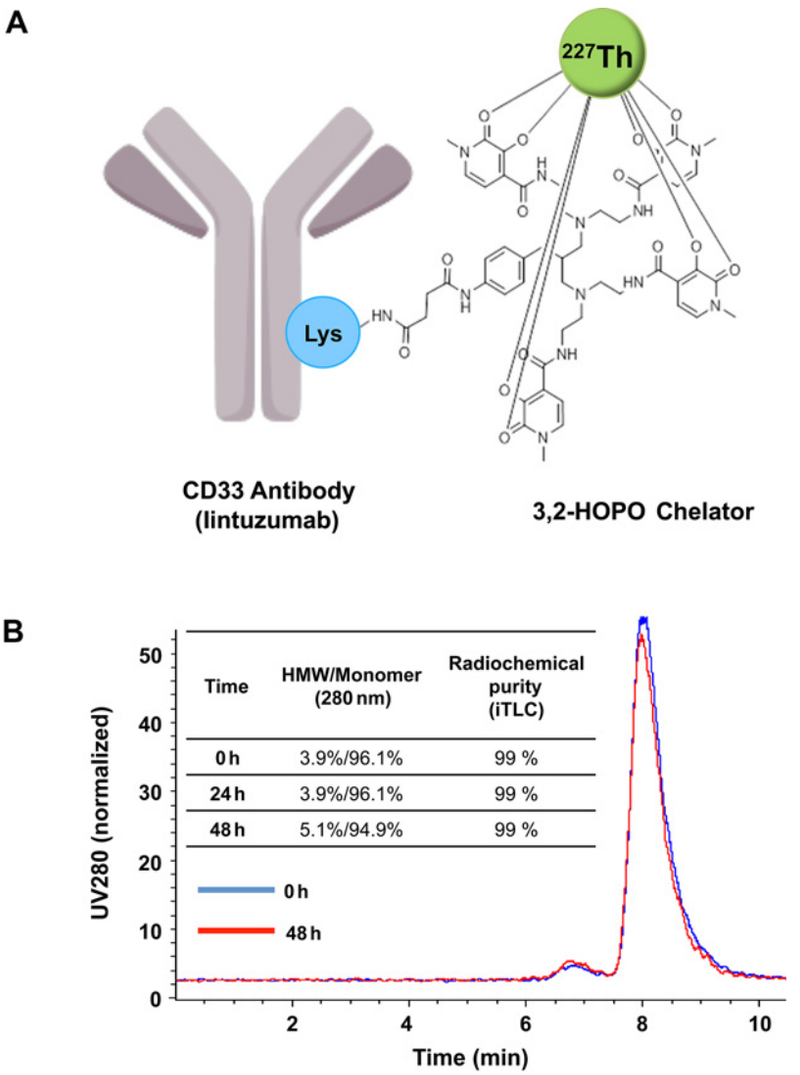

Figure 1.
Schematic sketch of CD33-TTC and analysis of radiolabeling properties. **A,** the CD33-TTC, consisting of the CD33 antibody lintuzumab, the octadentate 3,2-HOPO chelator covalently linked via amine coupling to the antibody, enabling radiolabeling with one ^{227}Th radionuclide per chelator. **B,** radiostability analysis of CD33-TTC upon storage for 48 hours at room temperature. High molecular weight (HMW) levels and radiochemical purity (RCP) was determined by iTLC at $t = 0$ hour, $t = 24$ hours, and $t = 48$ hours.

radiolabeled CD33-TTC bound to CD33 molecules in a bead-based assay (Fig. 2B). Furthermore, as described in the literature (17), the lintuzumab-based CD33-TTC was found to internalize at a 3.4-fold higher rate than an isotype control-TTC (Fig. 2C).

In vitro cytotoxicity of the CD33-TTC

The *in vitro* cytotoxicity of the CD33-TTC was tested on the CD33-positive cell lines HL-60 and KG-1. These two cell lines were determined to express approximately 16,000 and 7,800 receptors/cell, respectively, and differ in their multidrug efflux pump status (HL-60, MDR-negative; KG-1, MDR-positive). Exposure of cells to CD33-TTC demonstrated dose-dependent reduction of cell viability on both cell lines (Fig. 3A and B). The reduction in viability was specific to CD33-TTC as an isotype control-TTC did not decrease cell viability. In addition, CD33 antibody–chelator conjugate did not reduce cell viability, nor did treatment of CD33-negative cells Ramos with CD33-TTC (Fig. 3C), thus demonstrating the targeting specificity of the CD33-TTC.

We next investigated the mode of action of the CD33-TTC. Thorium-227 has been shown to induce DNA double-strand breaks (DSB) when complexed to other targeting moieties such as rituximab (39). Therefore, HL-60 cells were exposed to isotype control-TTC or CD33-TTC (activities of 20 kBq/mL). Induction of DNA DSBs in nonapoptotic cells, gated using an anti-caspase3 antibody, was measured by detection of phosphorylated H2AX (γ-H2AX) by FACS. Approximately 2% of cells cultured in medium stained positive for γ-H2AX, whereas approximately 10% of cells exposed to isotype control-TTC and approximately 40% of cells exposed to CD33-TTC stained positive for γ-H2AX (Fig. 3D).

Next, we evaluated the effect on the cell cycle after exposure of HL-60 cells to CD33-TTC by flow cytometry analysis. As presented in Fig. 3E, cells were found to enter the cell-cycle G_2 phase within 24 hours after exposure to CD33-TTC, which further increased 48 hours after exposure to CD33-TTC in comparison with cells cultured in medium. These results indicate that CD33-TTC induces G_2 cell-cycle arrest.

In vivo biodistribution of the CD33-TTC

The biodistribution of the CD33-TTC was evaluated in a subcutaneous HL-60 xenograft mouse model. An increase over time of ^{227}Th activity in the tumor was observed with an accumulated activity of approximately 1,500 Bq/g (corresponding to

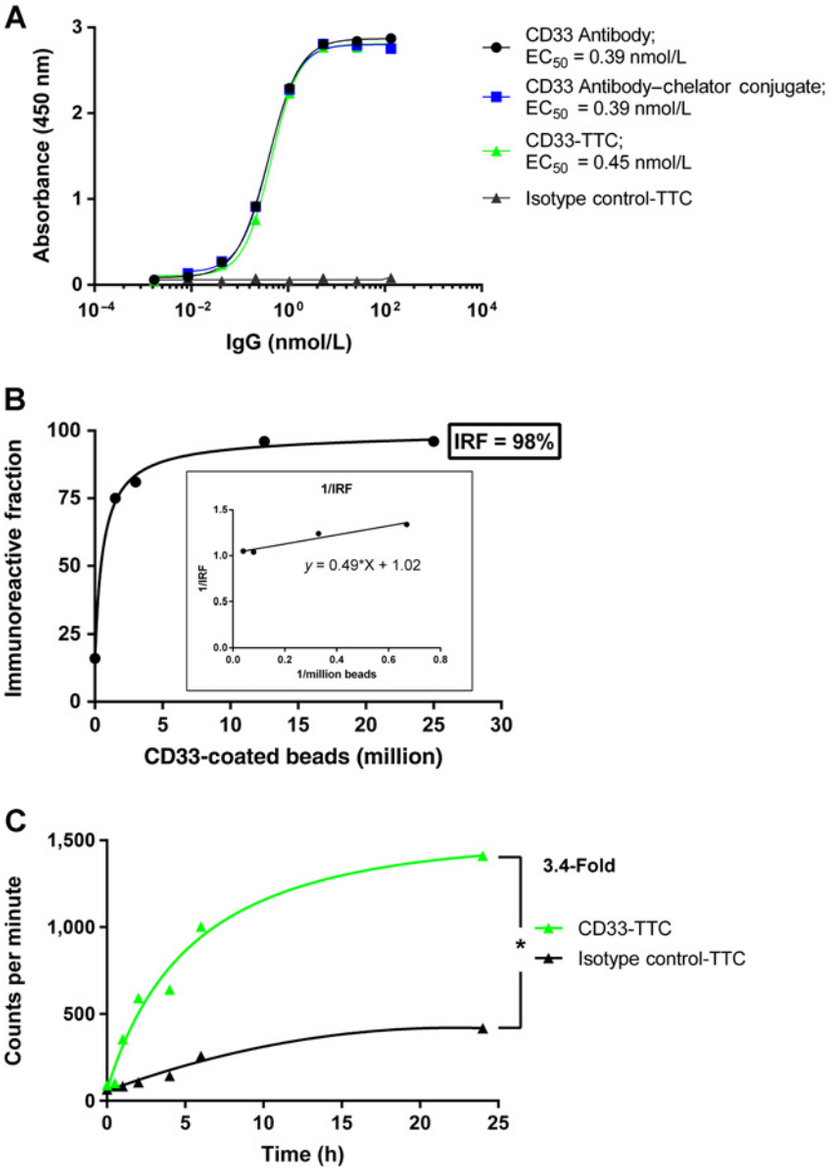

Figure 2.
Comparison of binding affinities using ELISA, determination of immunoreactive fraction (IRF) and internalization on HL-60 cells. **A,** ELISA to recombinant human CD33, comparing CD33 antibody, CD33 antibody–chelator conjugate, CD33-TTC, and an isotype control-TTC (TTCs radiolabeled at a specific activity of 50 kBq/μg). **B,** the IRF was determined upon incubation of the CD33-TTC on recombinant CD33-coated magnetic beads. The IRF was calculated to be 98% by linear regression after plotting the reciprocal of the determined IRF values against the increasing accessible target sites (1/million beads). **C,** internalization of CD33-TTC on HL-60 cells in comparison with an isotype control-TTC. The accumulated radioactivity (counts per minute) was determined at each individual time point. A 3.4-fold accumulation of the CD33-TTC over the isotype control-TTC was determined with statistical significance (unpaired *t* test).

22% of injected dose ^{227}Th per gram) on day 7 (Fig. 4A). The accumulation in the tumor was the reciprocal of the decrease of ^{227}Th in the blood and an activity of approximately 300 Bq/g of ^{227}Th per mL blood (corresponding to 5% of injected dose^{227}Th per gram) was determined on day 7. No major accumulation in any other organs was observed, which can be attributed to the lack of cross-reactivity of lintuzumab to murine CD33. The ^{223}Ra activity from decaying ^{227}Th was analyzed in parallel (Fig. 4B). A gradual increase of the ^{223}Ra activity in the tumor was observed with an accumulated activity of approximately 300 Bq/g on day 7. Similarly, increase of ^{223}Ra activity at a count of approximately 300 Bq/g was detected in the femur. In summary, high tumor accumulation of the CD33-TTC was demonstrated.

In vivo antitumor activity of the CD33-TTC

The antitumor activity of the CD33-TTC was evaluated *in vivo* in a subcutaneous HL-60 xenograft model. At the administered dose of 700 kBq/kg, complete tumor regression was observed, lasting for 20 days. Fifteen of 18 animals were free of any palpable tumors at the end of the study (Fig. 5A). In contrast, an isotype control-TTC administered at an equal radioactive dose showed no antitumor activity. Furthermore, tumor growth inhibition was dependent on the presence of ^{227}Th, as CD33 antibody–chelator conjugate lacked *in vivo* efficacy. No loss in body weight $\geq$10% was observed during the course of the study, demonstrating that the dose was well tolerated (Fig. 5B) which is in agreement with previous published data (40).

To further substantiate *in vivo* activity, CD33-TTC was evaluated in a disseminated HL-60 model. CD33-TTC was administered at radioactivity activities as indicated in Fig. 6. Dose-dependent efficacy of the CD33-TTC was observed (Fig. 6A) and median survival times (MST) of 90 days, 115.5 days, or undefined for animals receiving 50, 150, and 300 kBq/kg were calculated. In addition, animals receiving a fractionated dose of 2 × 150 kBq/kg

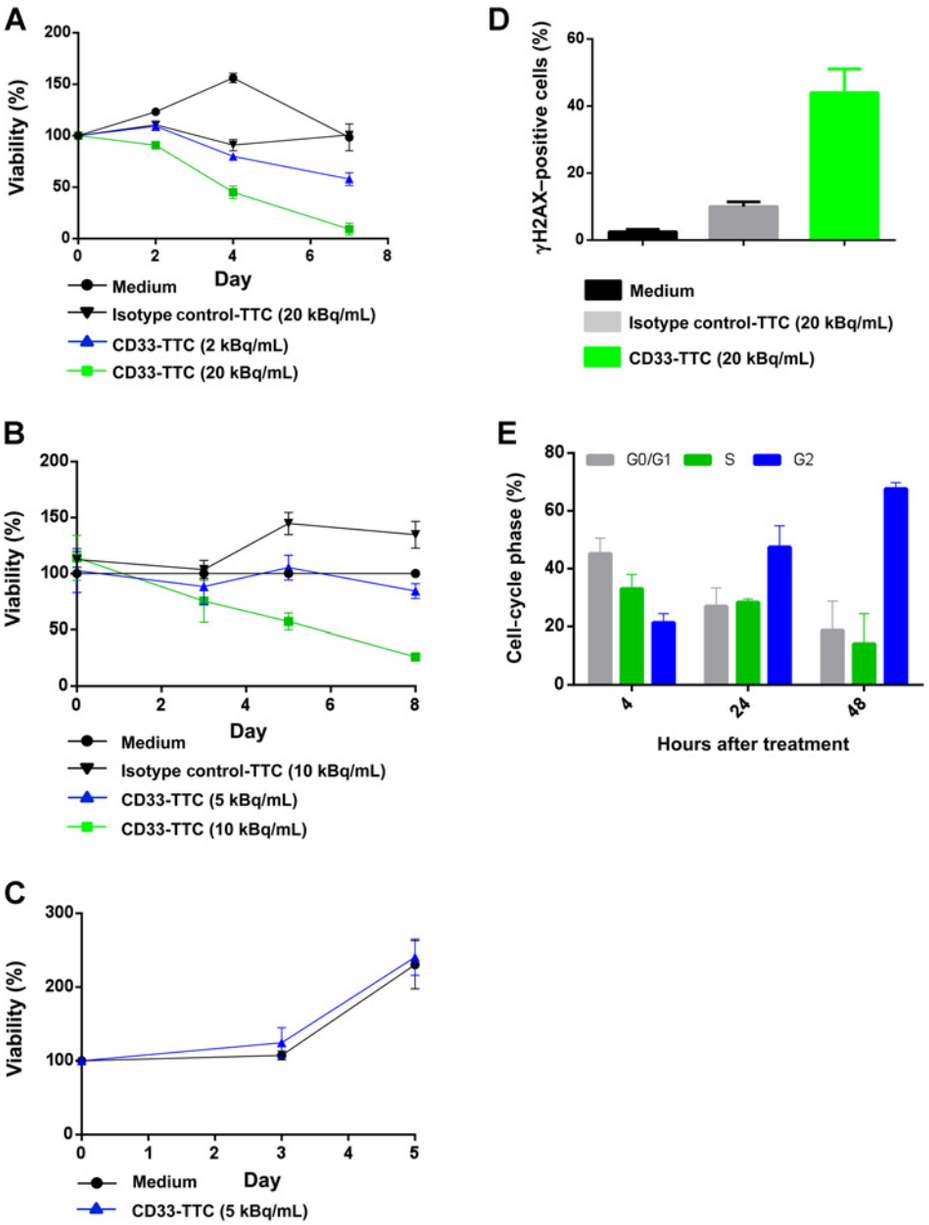

Figure 3.
In vitro cytotoxicity experiments of CD33-TTC and molecular analysis of mode of action. CD33- and isotype control-TTC were radiolabeled at 50 kBq/μg in all experiments. Cytotoxicity was evaluated by measuring cell viability. CD33-TTC and isotype control-TTC were incubated on cells at varying total activities in comparison with medium only. Measured cell viability on either MDR-negative HL-60 cells (**A**), MDR-positive KG-1 cells (**B**), or CD33-negative Ramos cells (**C**). **D,** determination of DNA double-strand breaks by detection of γ-H2AX protein in nonapoptotic cells using flow cytometry in medium, isotype control- and CD33-TTC–treated HL-60 cells. **E,** determination of cell-cycle phase using DRAQ7 staining and analysis by FACS at $t = 4$, 24, and 48 hours in HL-60 cells after exposure to CD33-TTC (total activity of 5 kBq/mL).

of CD33-TTC at an interim of two weeks had similar MST as a single dose of 300 kBq/kg of CD33-TTC. In contrast, MST of 55, 56, and 57 days for animals receiving vehicle, CD33 antibody–chelator conjugate, or an isotype control-TTC, respectively, were determined. All doses were well tolerated as judged by body weight measurements (Fig. 6B) and clinical blood chemistry. As presented, white and red blood cell counts measured at study day 67 (3.5 half-lives of ^{227}Th) and 123 (6.5 half-lives of ^{227}Th) were comparable with levels measured in animals treated with vehicle at study day −1 (Supplementary Fig. S3B). This is in agreement with previous published data (40), which demonstrate that ^{227}Th induces reversible myelosuppression.

Immunohistochemical analysis on diseased animals terminated at the humane endpoint revealed HL-60 positive tumors in kidneys and bone marrow (Supplementary Fig. S4) which were not present in animals treated with CD33-TTC, alive at the end of the study.

Discussion

There is an unmet medical need for the treatment of AML and CD33 is a validated target despite rather discouraging results from clinical trials in the past, including the withdrawal of Mylotarg. As such, SGN-CD33A is an ADC consisting of a humanized CD33 antibody that is armed with DNA cross-linking pyrrolobenzodiazepine dimers (PBD) which are released via a protease-cleavable linker. SGNCD33A demonstrated promising preclinical activity (8) and is currently being investigated in clinical trials. Similarly, IMGN779 (9) makes use of a new class of DNA alkylating agents called indolinobenzodiazepine pseudodimers (termed IGN) and

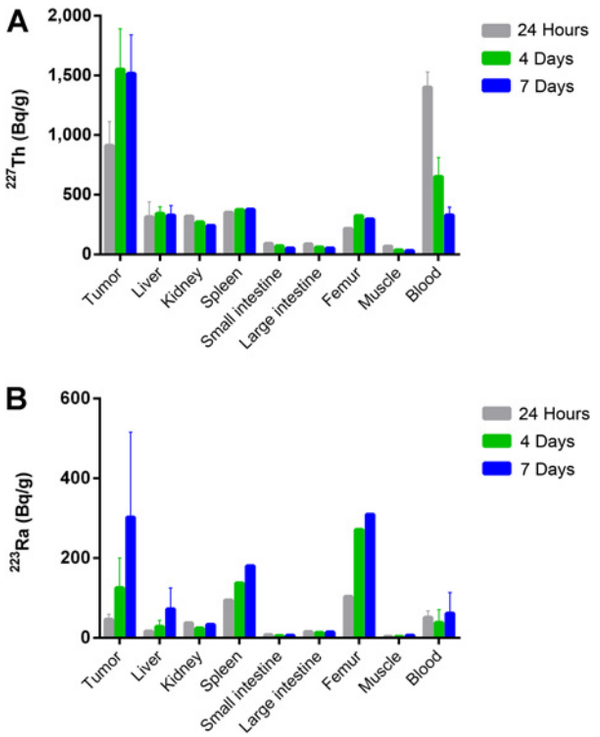

Figure 4.
Biodistribution of CD33-TTC in a subcutaneous HL-60 xenograft model. Biodistribution of CD33-TTC was analyzed 24 hours, 4 days, and 7 days after single intravenous dose administration (500 kBq/kg; 0.36 mg/kg). Accumulation of ^{227}Th (Bq/g; **A**) and ^{223}Ra (Bq/g; **B**) in tumors and organs, and decay corrected to timepoint of injection.

has recently entered clinical phase I. Another strategy being pursued includes the development of bispecific T-cell engaging molecules including BiTE AMG330 (10–13) and a recently developed tetravalent TandAb CD33/CD3 molecule (41). The development of BiTEs for the treatment of hematopoietic disorders might be promising as exemplified by blinatumomab, a CD19-CD3 BiTE, approved for the treatment of acute lymphoblastic leukemia (42).

The current study describes the development of a CD33-targeted thorium-227 conjugate (CD33-TTC), enabling the targeted delivery of ^{227}Th to CD33-positive cells. The data presented include detailed *in vitro* characterization and demonstrate robust *in vivo* antitumor activity of the CD33-TTC in subcutaneous and disseminated mouse models of AML.

In contrast to ADCs and T-cell engaging molecules, the efficacy of the CD33-TTC relies only on binding of the targeting moiety to the antigen, thereby delivering a toxic dose of radiation to the cells. With the purpose to not impair the initial binding event during manufacturing of the CD33-TTC, we have developed a conjugation and radiolabeling process that is performed at neutral pH and ambient temperatures. As demonstrated by ELISA, FACS, and IRF experiments, neither the conjugation nor the radiolabeling process impaired the binding properties to CD33 and the RCP was repeatedly ≥95%. In contrast, antibodies have been previously radiolabeled with ^{227}Th using *p*-SCN-Bn-DOTA, requiring conjugation of *p*-SCN-Bn-DOTA at a basic pH (pH 9) and subsequent radiolabeling with ^{227}Th for a minimum of 2 days at room temperature or at shorter periods at temperatures ≥60°C (43). Both of these steps are rather harsh with the increased likelihood of impairing the biological activity.

The mode of action (MoA) of the CD33-TTC was demonstrated to induce DNA double-strand breaks in cells. Furthermore, cells entered G_2 cell-cycle arrest and potentially apoptosis as observed by the detection of apoptotic bodies using microscopy (data not shown). This is in agreement with other studies using alpha-emitters as described for ^{213}Bi-labeled radioimmunoconjugates (44, 45). Furthermore, the CD33-TTC demonstrated reduction of *in vitro* viability on CD33-positive cell lines independent on the MDR status, potentially being an

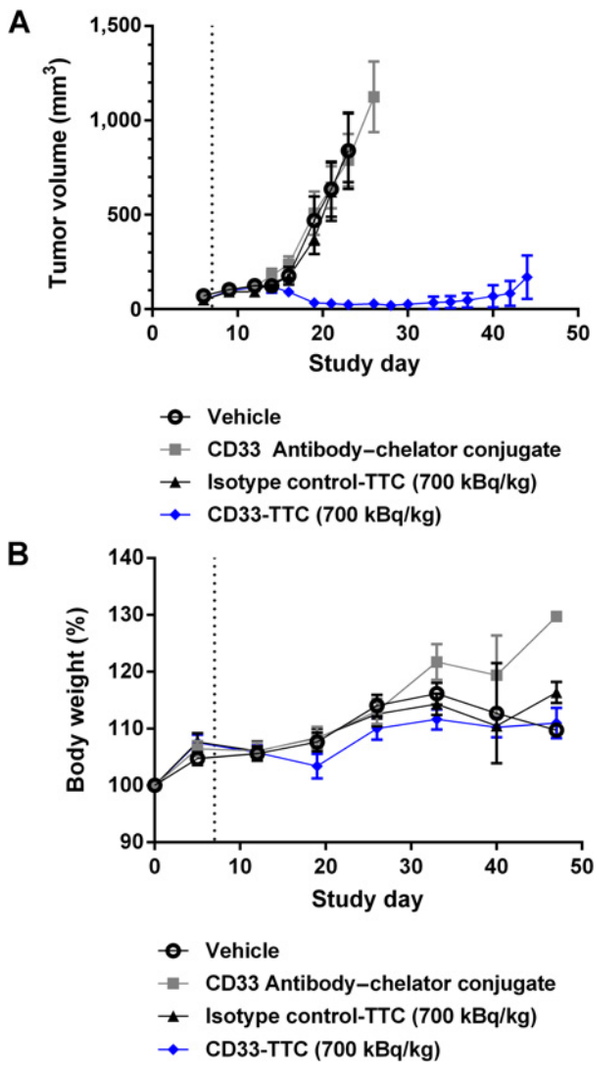

Figure 5.
In vivo efficacy of CD33-TTC in a subcutaneous HL-60 xenograft model. **A,** single dose injection of CD33-TTC or isotype control-TTC (radioactivite dose of 700 kBq/kg; protein dose of 0.36 mg/kg) in comparison with vehicle-treated or CD33 antibody–chelator conjugate–treated animals. Treatment start is indicated by the dashed line. Animals were sacrificed when the humane endpoint (tumor volume ≥ 1,500 mm^3) was reached. **B,** body weight measurements, expressed in percent during the course of the study.

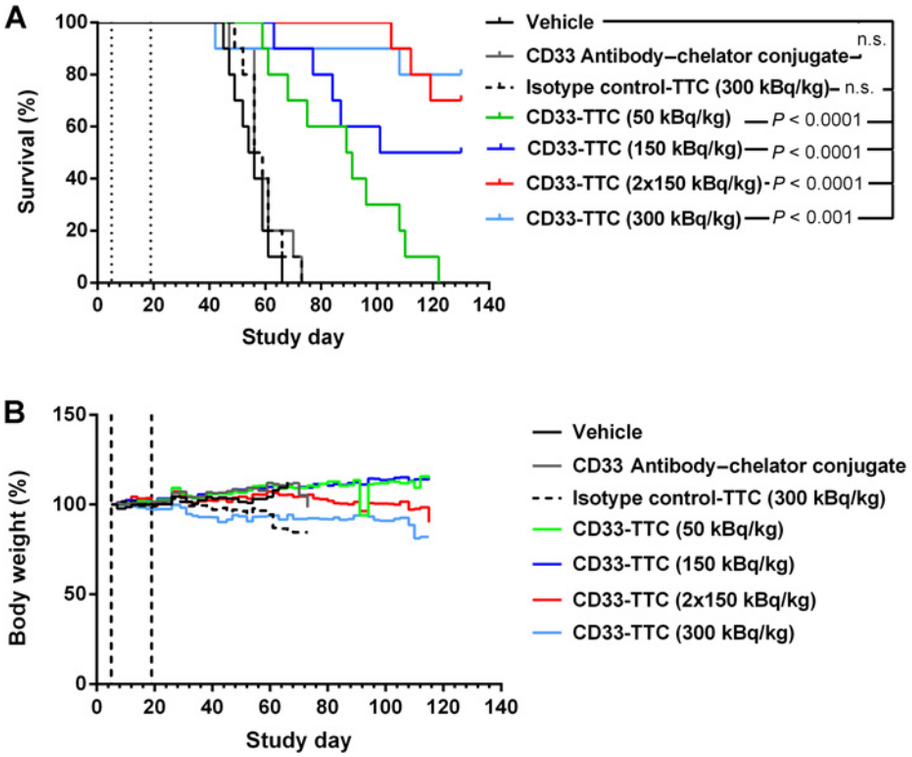

Figure 6.
In vivo efficacy of CD33-TTC in a disseminated HL-60 xenograft model. **A,** survival plot analysis of mice receiving CD33-TTC at the indicated dose levels in comparison with animals administered with vehicle, CD33 antibody–chelator conjugate or an isotype control-TTC. Dose administration (indicated by the dashed lines) was initiated five days after HL-60 cell inoculation. In a separate arm of the study, animals were administered twice with CD33-TTC at a dose of 150 kBq/kg on day 5 and day 19 (indicated with dashed lines). Mean survival times were calculated to be 55 days (vehicle), 56 days (CD33 antibody chelator–conjugate), 57 days (isotype control-TTC, 300 kBq/kg), 90 days (CD33-TTC, 50 kBq/kg), 115.5 days (CD33-TTC, 150 kbq/kg), or undefined (CD33-TTC, 2 × 150 and 300 kBq/kg) with statistical significance (Mantel–Cox analysis) between vehicle treated and the experimental groups as indicated (n.s., not significant). **B,** body weight measurements, expressed in percent during the course of the study.

advantage in AML patients which have developed resistance to standard-of-care treatment (46).

The observed reduction of viability in *in vitro* assays correlated with *in vivo* efficacy in a subcutaneous xenograft model. Treatment with a single dose of CD33-TTC stopped tumor growth as well as caused tumor regression in contrast to an isotype control-TTC. These findings were supported by the biodistribution of the CD33-TTC where a gradual increase of ^{227}Th activity in the tumor was observed. Similar, a gradual increase of ^{223}Ra activity was measured in femur. This accumulation in the femur can be explained by ^{227}Th decaying to ^{223}Ra, which is detached from the CD33-TTC and subsequently incorporated into the core bone structure (2, 47).

In addition to the subcutaneous model, we demonstrated efficacy of the CD33-TTC in a disseminated mouse model of AML, resembling more closely human AML disease. Dose dependency of the CD33-TTC was observed, resulting in prolonged median survival in comparison with respective control groups. The disseminated model was performed in SCID mice due to the biology of the model. However, SCID mice are reported to be more sensitive to ionizing radiation due to their reduced efficiency in repairing DNA double-strand breaks (48, 49). Furthermore, it has been previously described that the no-observed-adverse-effect-level (NOAEL) for ^{227}Th-radioimmunoconjugates is in between 200 and 300 kBq/kg (40) and the maximum tolerated activity ranges from 600 to 1,000 kBq/kg dependent on the mouse strain (Balb/C and nude). Therefore, the maximum applied activity in the disseminated model was 300 kBq/kg (SCID) and 700 kBq/kg in the subcutaneous model (nude). White and red blood cell counts of animals treated with CD33-TTC in the disseminated model had comparable levels as vehicle-treated animals and no other adverse signs of toxicity (loss of body weight) were observed. Similarly, the activity of 700 kBq/kg in nude mice (subcutaneous model) was well tolerated as judged by body weight measurements and is in agreement with previously published work (40). However, caution should be taken during a potential clinical dose escalation and myelosuppression should be monitored carefully.

Taken together, our results support the development of CD33-TTC for the treatment of AML. The optimized chelator chemistry allows conjugation and radiolabeling reactions under mild conditions. Thorium-227 has a half-life of 18.7 and can be produced in commercial quantities from an ^{227}Ac-generator. These features reduce logistical hurdles and can be adapted to other targeting moieties. As such, we have recently initiated a clinical trial to assess the safety and tolerability of a CD22-targeted thorium-227 conjugate (BAY1862864) in relapsed or refractory CD22-positive non-Hodgkin lymphoma (clinical trial number NCT02581878).

Disclosure of Potential Conflicts of Interest

No potential conflicts of interest were disclosed.

Authors' Contributions

Conception and design: U.B. Hagemann, K. Wickstroem, A.O. Shea, J. Karlsson, R.M. Bjerke, A.S. Cuthbertson

Development of methodology: U.B. Hagemann, K. Wickstroem, E. Wang, A.O. Shea, J. Karlsson, O.B. Ryan, A.S. Cuthbertson

Acquisition of data (provided animals, acquired and managed patients, provided facilities, etc.): K. Wickstroem, E. Wang, A.O. Shea

Analysis and interpretation of data (e.g., statistical analysis, biostatistics, computational analysis): U.B. Hagemann, K. Wickstroem, E. Wang, A.O. Shea, K. Sponheim, J. Karlsson, R.M. Bjerke, A.S. Cuthbertson

Writing, review, and/or revision of the manuscript: U.B. Hagemann, K. Wickstroem, E. Wang, A.O. Shea, J. Karlsson, R.M. Bjerke, A.S. Cuthbertson

Administrative, technical, or material support (i.e., reporting or organizing data, constructing databases): U.B. Hagemann, K. Wickstroem, E. Wang, J. Karlsson, R.M. Bjerke, O.B. Ryan
Study supervision: U.B. Hagemann, E. Wang, A.O. Shea, R.M. Bjerke, O.B. Ryan, A.S. Cuthbertson

Acknowledgments

We thank Lars Abrahamsen for scientific advice and contributions. We thank Cobra Biologics (Sweden) for manufacturing of the CD33 antibody, Synthetica for synthesis of the chelator, Pipeline Biotech for conducting the animal experiments, and Micromorph for assisting with immunohistochemistry.

The costs of publication of this article were defrayed in part by the payment of page charges. This article must therefore be hereby marked *advertisement* in accordance with 18 U.S.C. Section 1734 solely to indicate this fact.

Received April 29, 2016; revised July 31, 2016; accepted August 2, 2016; published OnlineFirst August 17, 2016.

References

1. Parker C, Nilsson S, Heinrich D, Helle SI, O'Sullivan JM, Fossa SD, et al. Alpha emitter radium-223 and survival in metastatic prostate cancer. N Engl J Med 2013;369:213–23.
2. Abou DS, Ulmert D, Doucet M, Hobbs RF, Riddle RC, Thorek DL. Whole-body and microenvironmental localization of radium-223 in naive and mouse models of prostate cancer metastasis. J Natl Cancer Inst 2016;108: pii: djv380.
3. Henriksen G, Hoff P, Larsen RH. Evaluation of potential chelating agents for radium. Appl Radiat Isot 2002;56:667–71.
4. Deschler B, Lubbert M. Acute myeloid leukemia: epidemiology and etiology. Cancer 2006;107:2099–107.
5. Rajvanshi P. Hepatic sinusoidal obstruction after gemtuzumab ozogamicin (Mylotarg) therapy. Blood 2002;99:2310–4.
6. Wadleigh M, Richardson PG, Zahrieh D, Lee SJ, Cutler C, Ho V, et al. Prior gemtuzumab ozogamicin exposure significantly increases the risk of veno-occlusive disease in patients who undergo myeloablative allogeneic stem cell transplantation. Blood 2003;102:1578–82.
7. Kadia TM, Ravandi F, Cortes J, Kantarjian H. New drugs in acute myeloid leukemia (AML). Ann Oncol 2016;27:770–8.
8. Kung Sutherland MS, Walter RB, Jeffrey SC, Burke PJ, Yu C, Kostner H, et al. SGN-CD33A: a novel CD33-targeting antibody-drug conjugate using a pyrrolobenzodiazepine dimer is active in models of drug-resistant AML. Blood 2013;122:1455–63.
9. Miller ML, Fishkin NE, Li W, Whiteman KR, Kovtun Y, Reid EE, et al. A new class of antibody-drug conjugates with potent DNA alkylating activity. Mol Cancer Ther 2016;15:1870–8.
10. Aigner M, Feulner J, Schaffer S, Kischel R, Kufer P, Schneider K, et al. T lymphocytes can be effectively recruited for *exvivo* and *invivo* lysis of AML blasts by a novel CD33/CD3-bispecific BiTE antibody construct. Leukemia 2013;27:1107–15.
11. Harrington KH, Gudgeon CJ, Laszlo GS, Newhall KJ, Sinclair AM, Frankel SR, et al. The broad anti-AML activity of the CD33/CD3 BiTE antibody construct, AMG 330, is impacted by disease stage and risk. PLoS One 2015;10:e0135945.
12. Krupka C, Kufer P, Kischel R, Zugmaier G, Lichtenegger FS, Kohnke T, et al. Blockade of the PD-1/PD-L1 axis augments lysis of AML cells by the CD33/CD3 BiTE antibody construct AMG 330: reversing a T-cell-induced immune escape mechanism. Leukemia 2016;30:484–91.
13. Laszlo GS, Gudgeon CJ, Harrington KH, Walter RB. T-cell ligands modulate the cytolytic activity of the CD33/CD3 BiTE antibody construct, AMG 330. Blood Cancer J 2015;5:e340.
14. Kenderian SS, Ruella M, Shestova O, Klichinsky M, Aikawa V, Morrissette JJ, et al. CD33-specific chimeric antigen receptor T cells exhibit potent preclinical activity against human acute myeloid leukemia. Leukemia 2015;29:1637–47.
15. Wang QS, Wang Y, Lv HY, Han QW, Fan H, Guo B, et al. Treatment of CD33-directed chimeric antigen receptor-modified T cells in one patient with relapsed and refractory acute myeloid leukemia. Mol Ther 2015;23: 184–91.
16. Griffin JD, Linch D, Sabbath K, Larcom P, Schlossman SF. A monoclonal antibody reactive with normal and leukemic human myeloid progenitor cells. Leuk Res 1984;8:521–34.
17. Caron PC, Co MS, Bull MK, Avdalovic NM, Queen C, Scheinberg DA. Biological and immunological features of humanized M195 (anti-CD33) monoclonal antibodies. Cancer Res 1992;52:6761–7.
18. Co MS, Avdalovic NM, Caron PC, Avdalovic MV, Scheinberg DA, Queen C. Chimeric and humanized antibodies with specificity for the CD33 antigen. J Immunol 1992;148:1149–54.
19. Sekeres MA, Lancet JE, Wood BL, Grove LE, Sandalic L, Sievers EL, et al. Randomized, phase 2b study of low-dose cytarabine and lintuzumab versus low-dose cytarabine and placebo in older adults with untreated acute myeloid leukemia. Haematologica 2013;98:119–28.
20. Borthakur G, Rosenblum MG, Talpaz M, Daver N, Ravandi F, Faderl S, et al. Phase 1 study of an anti-CD33 immunotoxin, humanized monoclonal antibody M195 conjugated to recombinant gelonin (HUM-195/rGEL), in patients with advanced myeloid malignancies. Haematologica 2013;98: 217–21.
21. Lapusan S. Phase I studies of AVE9633, an anti-CD33 antibody-maytansinoid conjugate, in adult patients with relapsed/refractory acute myeloid leukemia. Invest New Drugs 2012;30:1121–31.
22. Clift RA, Buckner CD, Appelbaum FR, Bearman SI, Petersen FB, Fisher LD, et al. Allogeneic marrow transplantation in patients with acute myeloid leukemia in first remission: a randomized trial of two irradiation regimens. Blood 1991;77:1660–5.
23. Kersemans V, Cornelissen B, Minden MD, Brandwein J, Reilly RM. Drug-resistant AML cells and primary AML specimens are killed by 111In-anti-CD33 monoclonal antibodies modified with nuclear localizing peptide sequences. J Nucl Med 2008;49:1546–54.
24. Linenberger ML. CD33-directed therapy with gemtuzumab ozogamicin in acute myeloid leukemia: progress in understanding cytotoxicity and potential mechanisms of drug resistance. Leukemia 2005;19: 176–82.
25. Tang R, Cohen S, Perrot J-Y, Faussat A-M, Zuany-Amorim C, Marjanovic Z, et al. P-gp activity is a critical resistance factor against AVE9633 and DM4 cytotoxicity in leukaemia cell lines, but not a major mechanism of chemoresistance in cells from acute myeloid leukaemia patients. BMC Cancer 2009;9:199.
26. Jurcic JG, Larson SM, Sgouros G, McDevitt MR, Finn RD, Divgi CR, et al. Targeted alpha particle immunotherapy for myeloid leukemia. Blood 2002;100:1233–9.
27. Burke JM, Caron PC, Papadopoulos EB, Divgi CR, Sgouros G, Panageas KS, et al. Cytoreduction with iodine-131-anti-CD33 antibodies before bone marrow transplantation for advanced myeloid leukemias. Bone Marrow Transplant 2003;32:549–56.
28. Supiot S, Faivre-Chauvet A, Couturier O, Heymann MF, Robillard N, Kraeber-Bodere F, et al. Comparison of the biologic effects of MA5 and B-B4 monoclonal antibody labeled with iodine-131 and bismuth-213 on multiple myeloma. Cancer 2002;94:1202–9.
29. Sgouros G, Ballangrud AM, Jurcic JG, McDevitt MR, Humm JL, Erdi YE, et al. Pharmacokinetics and dosimetry of an alpha-particle emitter labeled antibody: 213Bi-HuM195 (anti-CD33) in patients with leukemia. J Nucl Med 1999;40:1935–46.
30. Rosenblat TL, McDevitt MR, Mulford Da, Pandit-Taskar N, Divgi CR, Panageas KS, et al. Sequential cytarabine and alpha-particle immunotherapy with bismuth-213-lintuzumab (HuM195) for acute myeloid leukemia. Clin Cancer Res 2010;16:5303–11.
31. Jurcic J, Ravandi F, Pagel J. Phase I trial of the targeted alpha-particle nanogenerator actinium-225-lintuzumab (anti-CD33) in combination with low-dose cytarabine for older patients with untreated acute myeloid leukemia. Blood 2013;122:1460.
32. Jurcic JG, Rosenblat TL. Targeted alpha-particle immunotherapy for acute myeloid leukemia. Am Soc Clin Oncol Educ Book. 2014:e126-31. doi: 10.14694/EdBook_AM.2014.34.e126.
33. Ramdahl T, Bonge-Hansen HT, Ryan OB, Larsen A, Herstad G, Sandberg M, et al. Efficient chelator for complexation of thorium-227. Bioorg Med Chem Lett 2016;26:4318–21.

34. Kim YS, Brechbiel MW. An overview of targeted alpha therapy. Tumor Biol 2012;33:573–90.
35. Abbas N, Heyerdahl H, Bruland OS, Borrebaek J, Nesland J, Dahle J. Experimental alpha-particle radioimmunotherapy of breast cancer using 227Th-labeled p-benzyl-DOTA-trastuzumab. EJNMMI Res 2011;1:18.
36. Lindmo T, Boven E, Cuttitta F, Fedorko J, Bunn PAJr. Determination of the immunoreactive fraction of radiolabeled monoclonal antibodies by linear extrapolation to binding at infinite antigen excess. J Immunol Methods 1984;72:77–89.
37. Michel RB, Mattes MJ. Intracellular accumulation of the anti-CD20 antibody 1F5 in B-lymphoma cells. Clin Cancer Res 2002;8:2701–13.
38. Reddy N, Ong GL, Behr TM, Sharkey RM, Goldenberg DM, Mattes MJ. Rapid blood clearance of mouse IgG2a and human IgG1 in many nude and nu/+ mouse strains is due to low IgG2a serum concentrations. Cancer Immunol Immunother 1998;46:25–33.
39. Dahle J, Borrebaek J, Jonasdottir TJ, Hjelmerud AK, Melhus KB, Bruland OS, et al. Targeted cancer therapy with a novel low-dose rate alpha-emitting radioimmunoconjugate. Blood 2007;110:2049–56.
40. Dahle J, Jonasdottir TJ, Heyerdahl H, Nesland JM, Borrebæk J, Hjelmerud AK, et al. Assessment of long-term radiotoxicity after treatment with the low-dose-rate alpha-particle-emitting radioimmunoconjugate 227Th-rituximab. Eur J Nucl Med Mol Imaging 2010;37:93–102.
41. Reusch U, Harrington K, Gudgeon C, Fucek I, Ellwanger K, Weichel M, et al. Characterization of CD33/CD3 tetravalent bispecific tandem diabodies (TandAbs) for the treatment of acute myeloid leukemia. Clin Cancer Res. 2016 May 17. [Epub ahead of print].
42. Topp MS, Gökbuget N, Zugmaier G, Degenhard E, Goebeler ME, Klinger M, et al. Long-term follow-up of hematologic relapse-free survival in a phase 2 study of blinatumomab in patients with MRD in B-lineage ALL. Blood 2012;120:5185–7.
43. Heyerdahl H, Krogh C, Borrebaek J, Larsen A, Dahle J. Treatment of HER2-expressing breast cancer and ovarian cancer cells with alpha particle-emitting 227Th-trastuzumab. Int J Radiat Oncol Biol Phys 2011;79:563–70.
44. Friesen C, Roscher M, Hormann I, Leib O, Marx S, Moreno J, et al. Anti-CD33-antibodies labelled with the alpha-emitter Bismuth-213 kill CD33-positive acute myeloid leukaemia cells specifically by activation of caspases and break radio- and chemoresistance by inhibition of the anti-apoptotic proteins X-linked inhibitor o. Eur J Cancer 2013;49:2542–54.
45. Li Y, Cozzi PJ, Qu CF, Zhang DY, Rizvi SMA, Raja C, et al. Cytotoxicity of human prostate cancer cell lines *invitro* and induction of apoptosis using Bi-213-Herceptin alpha-conjugate. Cancer Lett 2004;205:161–71.
46. Cianfriglia M. The biology of MDR1-P-glycoprotein (MDR1-Pgp) in designing functional antibody drug conjugates (ADCs): the experience of gemtuzumab ozogamicin. Ann Ist Super Sanita 2013;49:150–68.
47. Shirley M, McCormack PL. Radium-223 dichloride: a review of its use in patients with castration-resistant prostate cancer with symptomatic bone metastases. Drugs 2014;74:579–86.
48. Fulop GM, Phillips RA. The scid mutation in mice causes a general defect in DNA repair. Nature 1990;347:479–82.
49. Biedermann KA, Sun JR, Giaccia AJ, Tosto LM, Brown JM. scid mutation in mice confers hypersensitivity to ionizing radiation and a deficiency in DNA double-strand break repair. Proc Natl Acad Sci U S A 1991;88:1394–7.